Spontaneous fission and α decay from K-isomeric states within a cluster approach

I. S. Rogov,[1,2] G. G. Adamian,[1] and N. V. Antonenko[1,2]
[1] Joint Institute for Nuclear Research, 141980 Dubna, Russia
[2] Tomsk Polytechnic University, 634050 Tomsk, Russia

(Received 28 May 2024; accepted 20 June 2024; published 8 July 2024)

Spontaneous fission and α decay from K-isomeric states are studied within the dinuclear system model. All these processes are considered as evolution of a nucleus in the charge (mass) asymmetry coordinate. For even-even and even-odd actinides and superheavy nuclei, the spontaneous fission and α-decay half-lives of K-isomeric states are calculated and compared with the available experimental data. The origin of the hindrance of spontaneous fission from the high-K isomeric states is explained.

DOI: 10.1103/PhysRevC.110.014606

I. INTRODUCTION

The nuclear K-isomers are the long-living excited states, which are of fundamental as well as application interest, particularly in the creation of nuclear lasers and new source of energy [1–21]. Much experimental information has already been accumulated on the partial widths of γ and α decays from isomeric states of heaviest nuclei [22–76]. Nucleus ^{250}No becomes, thus, one of the very few examples of heavy nuclei with the isomeric state living considerably longer than the ground state [26,29,43,51]. This "inversion" of stability indicates the significant role of high-K isomerism in the study of heavy and superheavy nuclei (SHN) [10,77–80] and opens up new possibilities for the production of SHN in the isomeric states [81].

The electromagnetic decay of isomeric states involves a large change in K value, leading to a significant lifetime, as a consequence the α decay and spontaneous fission (SF) branches become observable. For instance, K isomer in ^{270}Ds decays via α emission with notably long lifetime [79]. An analysis of experimental data [48,49] has established the existence of fissioning isomeric states in ^{244}Cm, ^{256}Fm, ^{251,254}No, ^{253,256,261}Rf, and ^{259}Sg. For ^{250}No, the SF activity of 36 μs was first reported in Ref. [26]. In Ref. [29], the decay of the $K^{\pi} = 6^{+}$ isomer in ^{250}No was associated with a fission activity having a half-life of 43^{+22}_{-15} μs, which is longer than that of the ground state, $3.7^{+1.1}_{-0.8}$ μs. From these data we cannot distinguish whether the isomer decays via SF directly or proceeds through a K-forbidden electromagnetic decay to the ground state, which goes to fission. In Ref. [43], a new internal transition branch was measured stemming from the isomeric state in ^{250}No which decays towards the ground state with a half-life of $34.9^{+3.9}_{-3.2}$ μs followed by the ground-state fission with a half-life of $3.8^{+0.3}_{-0.3}$ μs. The experimental arguments against SF from the lower-lying isomer of ^{250}No were given in Ref. [51]. The average multiplicities of prompt neutron emission in the SF corresponding to each SF activity in ^{250}No were measured for the first time in Refs. [42,54] to clarify if there is any evidence of K-isomer fission due to difference in prompt neutron multiplicity distributions. However, the proper analysis does not allow us to answer confidently the question whether the long-lived activity of ^{250}No is caused by the SF from K-isomer or from the ground state after electromagnetic transitions [42,54]. Note that the excitation-energy-dependent population probability of the low-lying isomer in ^{250}No was also studied in Ref. [53].

The longer half-life of the isomeric state compared to the ground state suggests that there is substantial fission hindrance (FH) because of the large value of K. Experimental and theoretical studies of this issue continue to be of interest for assessing the survival of superheavy nuclei. The existing experimental data suggest a FH mechanism for high-K isomers similar to that for odd-A or odd-odd nuclei in the whole actinide and SHN regions. Within the cluster model [82–84], the increased hindrance in fission of isomeric states can be attributed to the increased action through the fission barrier due to the large K. The spin dependence of total potential energy mainly modifies both the shape and height of the isomer fission barrier in comparison to the ground state fission barrier. Note that the main assumption of the cluster model is that charge asymmetry is a relevant collective coordinate for the SF process. This approach allows us to describe simultaneously the α decay, cluster radioactivity, and SF. The cluster model reproduces pretty well the global isotopic trends of SF, cluster radioactivity, and α-decay half-lives for even-even and even-odd nuclei Th, U, Pu, Cm, Cf, Fm, No, Rf, Sg, and Hs [82–84]. The half-lives of spontaneously fissioning nuclei with $Z \geqslant 110$ produced in the ^{48}Ca-induced complete fusion reactions with actinide targets are also well described and predicted within the cluster model [85–87].

The goals of the present work are to describe the SF and α-decay half-lives for the isomeric states and to understand the origin of the FH for these isomeric states within the cluster approach. An intriguing question is whether the proposed cluster approach is good for the isomeric states as well as for the ground state of even-even and even-odd nuclei. Calculations are performed for even-even and even-odd nuclei in the region of $96 \leqslant Z \leqslant 110$. Section II involves the method of calculations of SF and α-decay half-lives. In Sec. III, we present the results of calculations in the comparison with the available experimental data. Finally, we summarize our results in Sec. IV.

II. MODEL

Fission process is considered here within the dinuclear system (DNS) model [82–84] in which the formation of cluster with charge number $Z_L \geqslant 2$ is described as the evolution of the system in charge asymmetry coordinate $\eta_Z = (Z_H - Z_L)/(Z_H + Z_L)$. Here, Z_i (A_i), where $i = L, H$ is the charge (mass) number of the ith cluster and $Z = Z_L + Z_H$ ($A = A_L + A_H$) is the total charge (mass) number of the DNS. The $\eta_Z = 1$ corresponds to the state of mononucleus (clusterless nucleus), and $\eta_Z = 0$ is for the symmetric DNS configuration. The mass asymmetry coordinate $\eta = (A_H - A_L)/A$ is assumed to be strongly related to η_Z by the condition of the potential energy minimum. Indeed, at given η_Z the DNS potential energy as a function of η has a well-defined minimum. So, the spreading in η is small at each η_Z. The decay of the formed DNS is considered as a motion of the DNS in the relative distance R. Thus, the probability of finding two clusters L and H at given η_Z is proportional to the leakage of the ground-state wave function in R at this η_Z. To simplify the description of cluster decay [88–100], the process is usually divided into two independent stages: forming the cluster state or DNS, and its decay in R coordinate [100].

The probability of DNS formation (spectroscopic factor) S_L is determined by solving the stationary Schrödinger equation [82–84]

$$H\Psi_n(\eta_Z) = E_n\Psi_n(\eta_Z), \tag{1}$$

where the collective Hamiltonian

$$H = -\frac{\hbar^2}{2}\frac{\partial}{\partial\eta_Z}(B^{-1})_{\eta_Z}\frac{\partial}{\partial\eta_Z} + U(R_m, \eta_Z, \Omega) \tag{2}$$

contains the inverse inertia coefficient $(B^{-1})_{\eta_Z}$ and the potential energy U calculated at the touching distance $R = R_m$ at given η_Z. The model presented here belongs to the cluster type, because the ground state of the nucleus is assumed to have a small admixture of cluster-state components. Here the cluster state means two touching nuclei or a DNS. The total wave function $\Psi_n(\eta_Z)$ of the nucleus is expressed by a superposition of cluster and clusterless components. Since we assume that the spin and parity of the fissioning nucleus are preserved during SF, all cluster and clusterless components have the same spin and parity as in the parent nucleus. These effects are effectively described through the inclusion of the centrifugal potential in the DNS potential energy [101]

$$U(R_m, \eta_Z, \Omega) = V(R_m, \eta_Z, \Omega) + (Q_L + Q_H - Q_M), \tag{3}$$

which, as a function of charge asymmetry, is referred to a driving potential. Here, Q_M and $Q_{L,H}$ are the experimental mass excesses [102] of the parent nucleus and the nuclei forming the DNS, respectively. If the experimental mass excesses are not available, we take the theoretical values from Refs. [12,103,104]. The energy of isomeric state is taken into account in Q_M. The peculiarities of structure of the DNS nuclei are taken into account through $Q_{L,H}$. The tip-tip orientation of axial symmetric deformed nuclei is taken in the calculations of driving potentials because it provides the minimum of the potential energy of the DNS considered. The nucleus-nucleus interaction potential

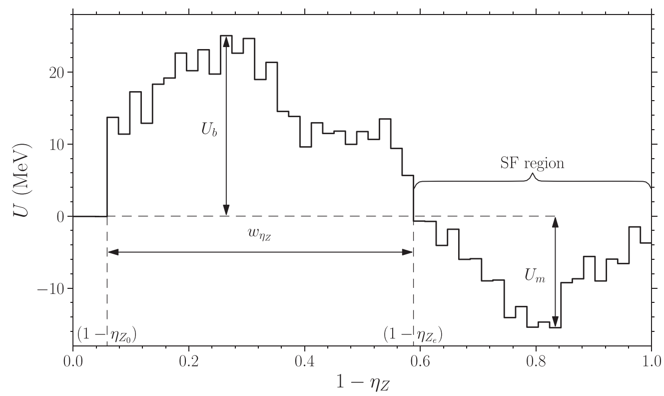

FIG. 1. Driving potential for ^{258}No. The fission barrier in η_Z is characterized by the height U_b and the width w_{η_Z}. The depth of the global potential minimum in the SF region is denoted by U_m. The tip-tip orientation of nuclei is taken in the DNS.

$$V(R, \eta_Z, \Omega) = V_C(R, \eta_Z) + V_N(R, \eta_Z) + V_r(R, \eta_Z, \Omega) \tag{4}$$

in Eq. (3) consists of the Coulomb V_C, nuclear V_N, and centrifugal V_r parts. The nuclear part V_N of the interaction potential is calculated in the double folding form, where the density-dependent nucleon-nucleon forces are folded with the nucleon densities of heavy and light nuclei of the DNS [82–84]. The centrifugal potential is calculated as

$$V_r = \hbar^2\Omega(\Omega+1)/(2\Im), \tag{5}$$

where Ω is the spin of fissioning nucleus and $\Im = c_1(\Im_L + \Im_H + \mu R_m^2)$ is the moment of inertia of the DNS ($\Im_{L,H}$ are rigid body moments of inertia for the clusters of the DNS, $c_1 = 0.85$ for all considered fissioning nuclei [99,100,105], and $\mu = m_0 A_L A_H/A$ is the reduced mass parameter (m_0 is the nucleon mass)). Note that the nucleus-nucleus potential depends on the ground-state quadrupole deformations [69,104,106] of the DNS nuclei and has a minimum at $R = R_m(\eta_Z, \Omega)$ [82–84].

The driving potential for the fissioning nucleus ^{258}No is shown in Fig. 1. The values of U and $(B^{-1})_{\eta_Z}$ are extended to the segments of the width $2\Delta = 2/Z$ so that the points η_Z are placed in the middle of the corresponding segments. The only exception is the mononucleus, for which we set $\eta_Z \in (1 - 4\Delta, 1]$ and the α-particle DNS with $\eta_Z \in (1 - 5\Delta, 1 - 4\Delta]$. The SF mainly occurs from the DNS configurations corresponding to the minima of the driving potential with energies smaller than the ground-state energy [82–84], i.e., at about $1 - \eta_Z > 0.6$. To undergo SF through the energy-resolved region with the global potential minimum of the depth U_m at $\eta_Z \approx 0.2$, the fissioning nucleus should penetrate the barrier of height U_b and width w_{η_Z} (Fig. 1). The values $1 - \eta_{Z_0}$ and $1 - \eta_{Z_e}$ are the entrance and exit turning points, respectively. Note that SF events occurs also from the sub-barrier region

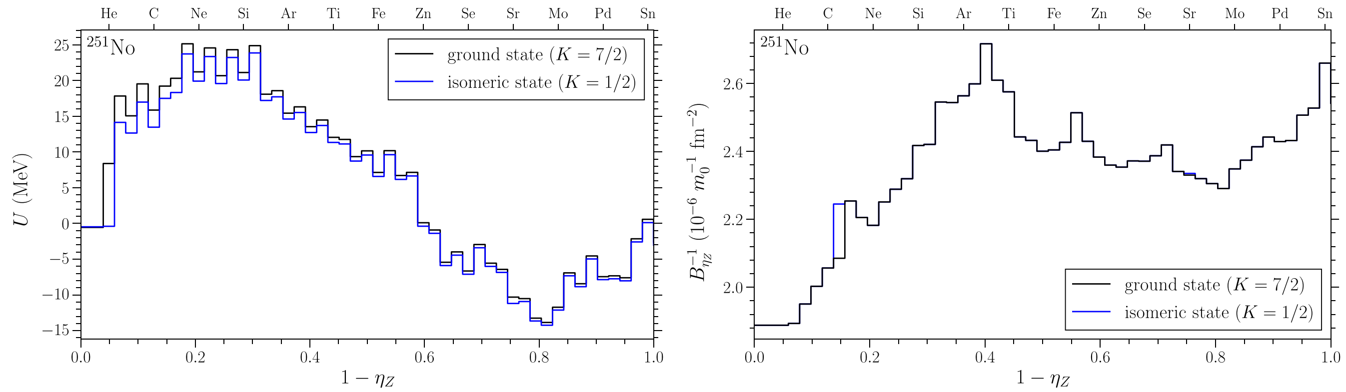

FIG. 2. Calculated driving potential U and inverse mass parameter $(B^{-1})_{\eta_Z}$ as the step functions of $1 - \eta_Z$ for the ground ($7/2^+$) and isomeric ($1/2^+$) states of ^{251}No. The light nuclei of the DNS are indicated on the upper horizontal axes.

but their contributions are negligible compared to the contributions from the energy-resolved region.

The preformation probability S_L of the DNS with certain charge number Z_L of light cluster is defined as

$$S_L = \int_{\eta_Z(Z_L)-\Delta}^{\eta_Z(Z_L)+\Delta} |\Psi_0(\eta_Z)|^2 d\eta_Z. \tag{6}$$

For the α decay and cluster radioactivity in the potential barrier region at about $1 - \eta_Z \leqslant 0.6$ (Fig. 1), the half-life is calculated as

$$T_{1/2}^{\alpha,\mathrm{cl}} = \frac{\hbar \ln 2}{\Gamma_L} = \frac{\pi \ln 2}{\omega_0 S_L P_L}, \tag{7}$$

where Γ_L is the decay width and P_L is the penetration probability of the α-particle or cluster through the Coulomb barrier calculated in the WKB approach [82–84]. The value of frequency ω_0 of zero-point vibration in η_Z coordinate near the mononucleus state ($\eta_Z \approx 1$) is equal to the distance between the ground and the first excited state of DNS vibrating in η_Z. In the case of SF, all DNS configurations in the SF region contribute because their decay probabilities P_L in R coordinate are equal to 1. Therefore, the SF half-life is calculated as

$$T_{1/2}^{\mathrm{sf}} = \frac{\pi \ln 2}{\omega_0 S_{\mathrm{sf}}}, \tag{8}$$

where

$$S_{\mathrm{sf}} = \int_0^{\eta_{Z_e}} |\Psi_0(\eta_Z)|^2 d\eta_Z \tag{9}$$

and η_{Z_e} is the exit turning point (see Fig. 1). Note that the ground state wave function Ψ_0 of Eq. (1) is used in Eqs. (6) and (9).

III. SF AND α DECAY FROM K-ISOMERIC AND GROUND STATES

The K-isomeric states are characterized by two parameters: spin projection K and energy E. The value of spin $\Omega = K$ is taken directly into consideration in the rotational part (5) of the driving potential. The energy E of isomeric state is introduced as an addition to the mass excess Q_M of the parent nucleus in Eq. (3).

In even-odd nuclei, the energies E of K-isomeric states are small ($\leqslant 200$ keV for nuclei considered), therefore, the hindrance factors of SF from the K-isomeric and ground states have the same origin. With growing value of K, there is an increase in the half-life and vice versa. Figures 2 and 3 show a comparison of the driving potentials for the ground and isomeric states of ^{251}No and ^{253}Rf. For both No and Rf, the spin of the ground state is higher than that for the isomeric

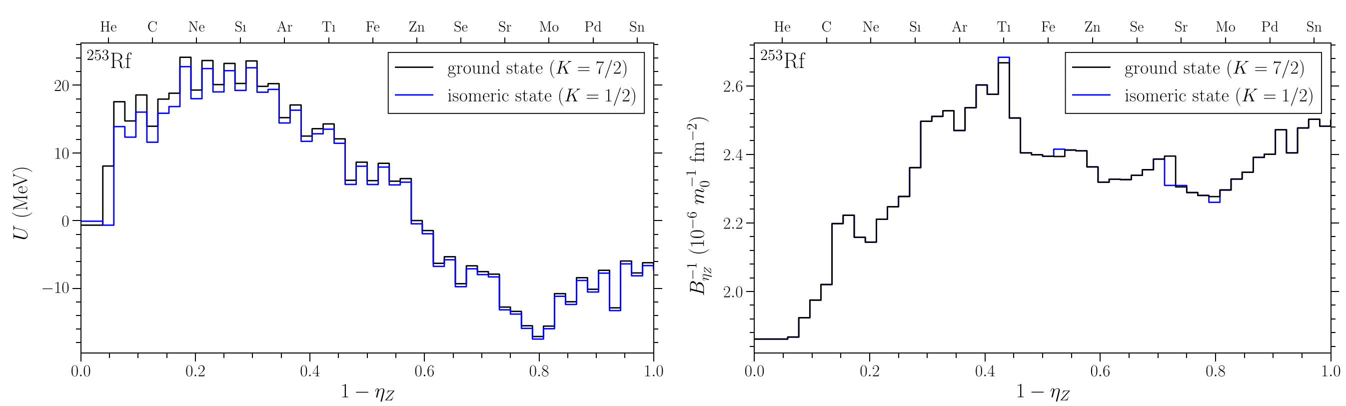

FIG. 3. The same as described in the caption of Fig. 2, but for ^{253}Rf.

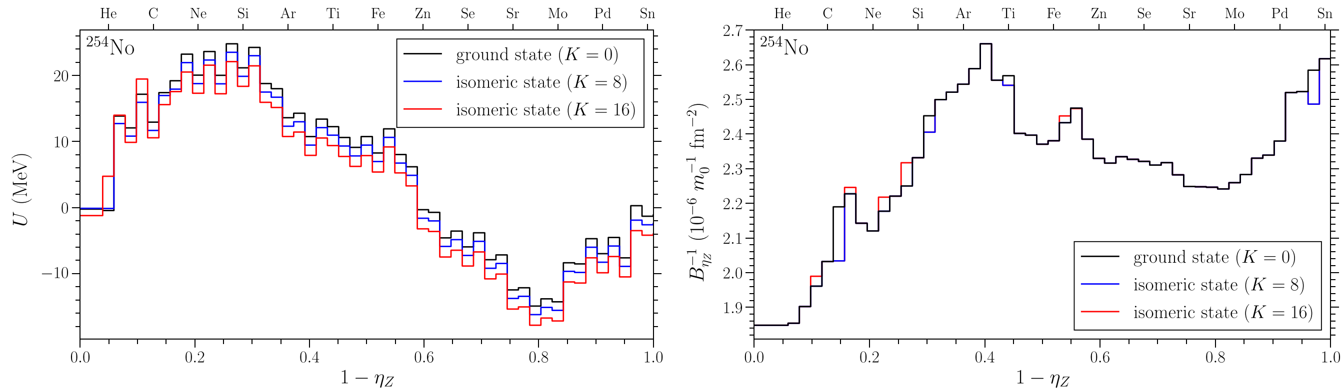

FIG. 4. Calculated driving potential U and inverse mass parameter $(B^{-1})_{\eta_Z}$ as the step functions of $1 - \eta_Z$ for the ground 0^+ and isomeric (8^-), (16^+) states of ^{254}No. The light nuclei of the DNS are indicated on the upper horizontal axes.

state. As a result, in the region of the potential barrier the values of U for the ground state are higher than those for the K-isomeric state. As a result, the half-life of the ground state is expected to be larger than one of K-isomer.

In the case of even-even nuclei, the energies of K-isomeric states are much more "weighty" and are on the order of MeV or several MeV. In this case, the actions of the spin and energy on the isomer half-life are opposite. Nonzero value of K increases the driving potential, mainly in the area of the most asymmetric configurations. With growing $1 - \eta_Z$ the influence of $K \neq 0$ on the driving potential becomes less noticeable. The energy E of isomeric state affects the full driving potential, lowering it over the entire region of η_Z. Thus, the energy of isomeric state weakens the effect of the growth of the driving potential with spin and reduces the potential barrier in η_Z, as well as lowers the potential pocket in the region of SF. As a result, the effect of spin can be overcompensated by the effect of energy, which eventually leads to the fact that the SF from the K-isomeric state proceeds easier than from the ground state. Figures 4 and 5 show the driving potentials for the ground and isomeric states of ^{254}No and ^{254}Rf. As seen, the driving potential for ^{254}No at $K = 8$ is lower than the one at $K = 0$ almost in the entire region of η_Z, which leads to a decrease in the half-life of the isomeric state. The driving potential at $K = 16$ turns out to be higher than the one at $K = 0$ only in a small region of $0.04 < 1 - \eta_Z < 0.12$ that is not enough to overcompensate the effect of energy. As a result, the wave function penetrates easier into the region of SF ($1 - \eta_Z \geqslant 0.6$) than in the case of $K = 0$. For ^{254}Rf (Fig. 5), the driving potentials at $K = 8$ and 16 are also lower than that at K=0 almost in the entire region of η_Z. However, the energies of the mononucleus at $K = 8$ and 16 turn out to be significantly lower than the one at $K = 0$ (which differs from ^{254}No). A deeper minimum in this area "pulls-back" the density of the wave function into the region of mononucleus and does not allow the reduction of the driving potential to be fully realized. A smaller density of the wave function in the region of SF leads to an increase in the half-life compared to the ground state.

Since the mass parameters for ground and isomeric states are close in magnitude, the role of mass parameter in the FH is weaker than the role of potential energy. As an example, for ^{251,254}No and ^{253,254}Rf, we show in Figs. 2–5 the mass parameters of the ground and isomeric states.

The rate of $T_{1/2}$ growth with increasing (decreasing) K (E) at a fixed E (K) is shown in Figs. 6 and 7. As seen, an increase of energy of the K-isomeric state leads to a decrease in its half-life, both for α decay and SF. On the contrary, the

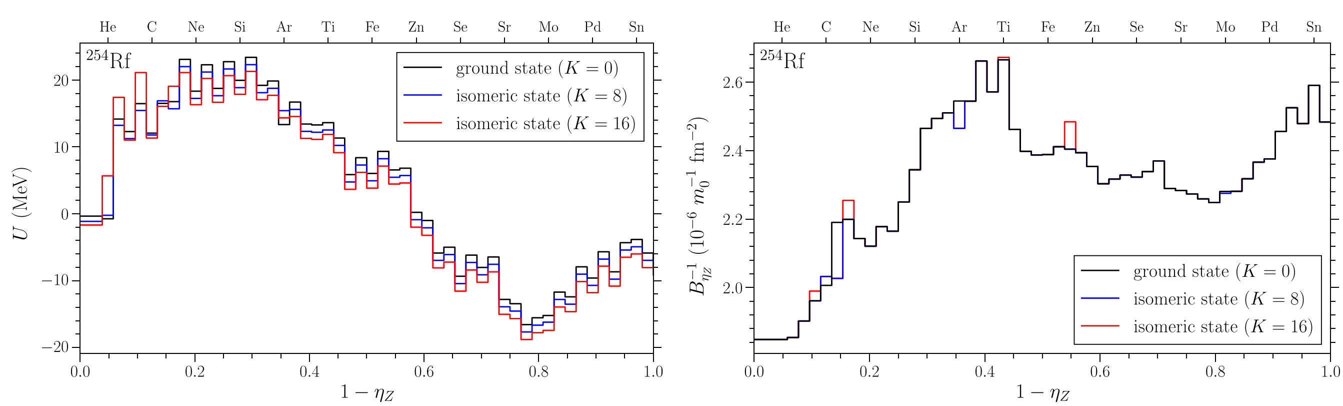

FIG. 5. The same as described in the caption of Fig. 4, but for ^{253}Rf.

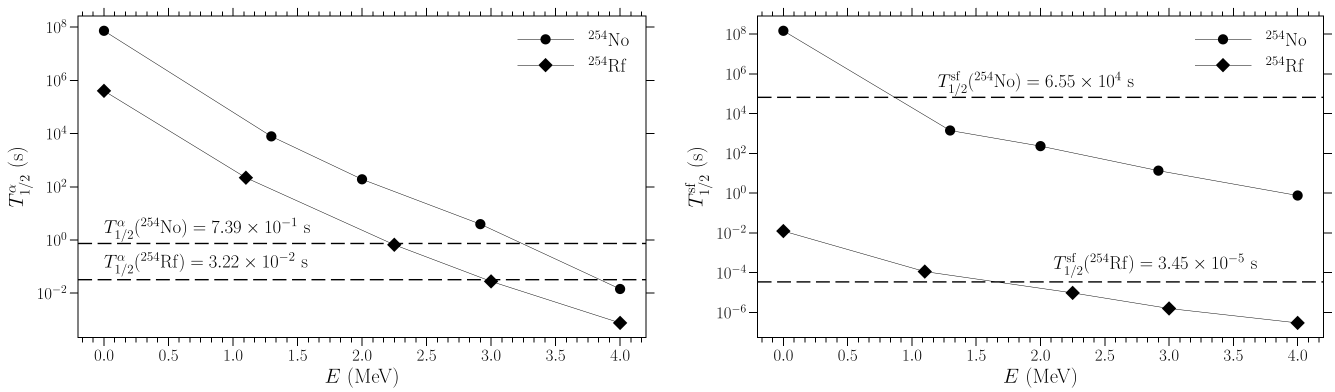

FIG. 6. Calculated half-lives for α decay and SF depending on the energy E of the isomeric state of ^{254}No (closed circles connected by lines) and ^{254}Rf (closed diamonds connected by lines) at $K = 8$. The dashed lines show the experimental α-decay and SF half-lives of the ground state for the indicated nuclei.

growth of K leads to an increase in the half-lives for both processes considered. Note that for α decay, the dependencies turn out to be somewhat closer to exponential than for SF because a change in the driving potential has a small effect on the probability of formation (S_α) of a system containing an α-particle, and the value of $T^{\alpha}_{1/2}$ is mainly affected by K and E through the penetrability in R.

As seen in Tables I–III, the calculated half-lives of even-even and even-odd nuclei are consistent with the available experimental data for SF and α decay from the ground and isomeric states. Note that our model also describes well the SF half-lives of even-even and even-odd actinides and SHN from the ground state [82–86]. It seems that theory is able to estimate unknown values of SF half-lives. The calculated results strongly depend on a nucleus considered. For example, for the isomeric states of even isotopes of No, there is an increase of SF half-life with number of neutrons and $T^{\alpha}_{1/2} > T^{\mathrm{sf}}_{1/2}$. For the isomeric states of even-odd nuclei, we have $T^{\alpha}_{1/2} < T^{\mathrm{sf}}_{1/2}$ with only the one exception for ^{255}Rf, where $T^{\alpha}_{1/2}$ and $T^{\mathrm{sf}}_{1/2}$ are comparable. In ^{254}No, there are isomers with $K = 8$, $E = 1.297$ MeV and $K = 16$, $E = 2.917$ MeV and the ratio $T^{\mathrm{sf}}_{1/2}(K = 16)/T^{\mathrm{sf}}_{1/2}(K = 8) \approx 6$ (Table I). In the case of ^{254}Rf, where $E = 1.1$ and 2.25 MeV at $K = 8$ and 16, respectively, the ratio $T^{\mathrm{sf}}_{1/2}(K = 16)/T^{\mathrm{sf}}_{1/2}(K = 8) \approx 10^3$ (Table I). The large difference between these ratios in ^{254}No and ^{254}Rf is due to the energy $\Delta E = E(K = 16) - E(K = 8)$ difference in both nuclei: $\Delta E \approx 1.60$ and 1.15 MeV in ^{254}No and ^{254}Rf, respectively. We find that the SF half-life of the $K^\pi = 6^+$ isomer in ^{250}No is comparable with that of the ground state (within a factor of 2) and the half-life of the internal γ-transition to the ground state [43,51,53]. Because of this fact we are not able to distinguish whether the isomer decays via SF directly or proceeds through a K-forbidden electromagnetic decay to the ground state, which then goes to fission. The SF half-life of the second $K^\pi = 16^+$ isomer in ^{250}No is predicted about 1.5 μs. The isomeric states of ^{254}Rf are more stable against the SF than the ground state (Table I). As seen in Table II, for the SHN ^{266}Hs and ^{270}Ds, the half-lives of the isomeric and ground states are almost comparable. Note that the isomer $K = 6$ in ^{270}Ds [61] is a possible isomeric state observe in the experiment [10,13,21].

In even-odd nuclei, the energies of the ground and isomeric states are close and the difference in $T^{\mathrm{sf}}_{1/2}$ of these states mainly arises from the difference in K. Accordingly, if K

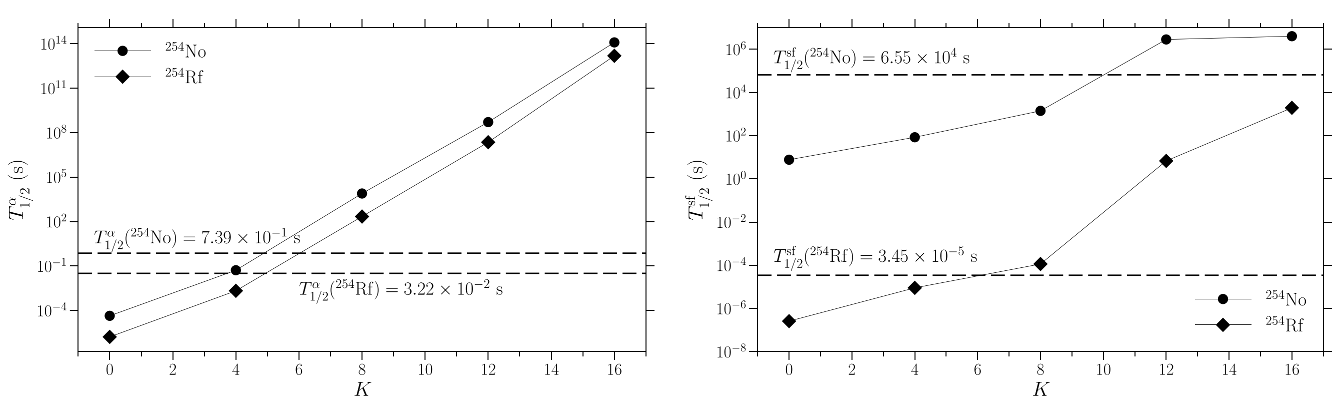

FIG. 7. Calculated half-lives for α decay and SF depending on the value of K of the isomeric state for ^{254}No at $E = 1.297$ MeV (closed circles connected by lines) and for ^{254}Rf at $E = 1.1$ MeV (closed diamonds connected by lines). The dashed lines show the experimental α-decay and SF half-lives of the ground state for the indicated nuclei.

TABLE I. The calculated (th.) and experimental (exp.) SF ($T^{sf}_{1/2}$) and α-decay ($T^{\alpha}_{1/2}$) half-lives for the ground states ($E = 0$) and K-isomers with the excitation energies E in even-even nuclei. The calculated spectroscopic factors S_α for the α-particle are also presented. The experimental data are either from Ref. [12] or indicated references.

Nucleus	K^π	E (MeV)	S_α	$T^{\alpha}_{1/2}$ (th.) (s)	$T^{\alpha}_{1/2}$ (exp.) (s)	$T^{sf}_{1/2}$ (th.) (s)	$T^{sf}_{1/2}$ (exp.) (s)
^{244}Cm	0^+	0	5.15×10^{-2}	3.06×10^{8}	7.50×10^{8}	3.13×10^{14}	4.17×10^{14}
^{244}Cm	6^+	1.042	4.28×10^{-2}	1.05×10^{9}		1.50×10^{9}	
^{250}Fm	0^+	0	5.99×10^{-2}	1.06×10^{3}	2.00×10^{3}	2.86×10^{7}	2.52×10^{7}
	(8^-)	1.199	3.89×10^{-2}	3.39×10^{5}		2.63×10^{4}	
^{256}Fm	0^+	0	6.56×10^{-2}	3.23×10^{5}	1.20×10^{5}	2.10×10^{4}	1.04×10^{4}
	7^-	1.425	3.95×10^{-3}	6.23×10^{6}		3.6×10^{-1}	$8^{+88}_{-7} \times 10^{-4}$ [24]
^{250}No	0^+	0	7.60×10^{-2}	1.85×10^{-3}	$>2.1 \times 10^{-4}$	12.0×10^{-6}	$3.7^{+1.1}_{-0.8} \times 10^{-6}$ [29]
							$3.8^{+0.3}_{-0.3} \times 10^{-6}$ [43]
							$4.0^{+4}_{-4} \times 10^{-6}$ [51]
							4.7×10^{-6} [53]
	(6^+)	1.050	6.14×10^{-3}	12.0		22.0×10^{-6}	$43^{+22}_{-15} \times 10^{-6}$ [29]
							$>34.9^{+3.9}_{-3.2} \times 10^{-6}$ [43]
							$>40 \times 10^{-6}$ [51]
	(16^+)	2.3	1.13×10^{-2}	6.4		1.3×10^{-6}	$\geqslant 0.7^{+1.4}_{-0.3} \times 10^{-6}$ [51]
^{252}No	0^+	0	7.07×10^{-2}	15.8	56.7	29.4	9
	(8^-)	1.255	5.30×10^{-2}	2.18×10^{3}		2.05×10^{-1}	
	(16^+)	2.7	7.72×10^{-2}	2.89×10^{2}		1.71×10^{-4}	
^{254}No	0^+	0	6.50×10^{-2}	7.39×10^{-1}	2.93	6.55×10^{4}	2.88×10^{4}
	(8^-)	1.297	3.10×10^{-3}	7.84×10^{3}	2.80×10^{3}	1.41×10^{3}	1.40×10^{3}
							$>4.70 \times 10^{3}$ [55]
	(16^+)	2.917	1.99×10^{-2}	1.47×10^{6}		8.36×10^{3}	$\geqslant 1.65$
^{254}Rf	0^+	0	8.07×10^{-2}	3.22×10^{-2}	$>1.55 \times 10^{-3}$	3.45×10^{-5}	2.30×10^{-5}
	(8^-)	1.10	5.77×10^{-2}	2.19×10^{2}		1.14×10^{-4}	$>4.70 \times 10^{-5}$
	(16^+)	2.25	2.63×10^{-2}	5.38×10^{4}		1.36×10^{-1}	$>6.02 \times 10^{-4}$
^{256}Rf	0^+	0	7.76×10^{-2}	2.11	2.08	4.98×10^{-3}	6.40×10^{-3}
	(7^-)	1.40	9.20×10^{-2}	8.46×10^{1}		1.78×10^{-5}	$1.4^{+0.6}_{-0.4} \times 10^{-5}$ [47]
	(13^-)	2.42	8.74×10^{-2}	3.13		1.29×10^{-6}	

of the isomer is larger than K of the ground state, then $T^{sf}_{1/2}$ (isomer)$>$ $T^{sf}_{1/2}$ (ground state), that is, the isomeric state is more stable with respect to SF. The prominent examples of this behavior are found in ^{257,261}Rf (Table III). If in this case $T_\gamma > T_{1/2}$ (isomer), then the isomer becomes the most stable nuclear state with respect to all decay modes and lives longer than the ground state. In nuclei ^{243}Cm, ^{249,251}No, ^{253,255}Rf, and ^{265}Sg, K (isomer)$<$ K_{gs} and $T^{sf}_{1/2}$ (isomer)$<$ $T^{sf}_{1/2}$ (ground state) (Table III).

For the isomeric states ($K < 10$) of even-even and even-odd nuclei, the SF half-lives can be parameterized as

$$T^{sf-K}_{1/2} = T^{sf\text{-}gs}_{1/2} \exp\left[\frac{c_1 E + c_2 \Delta K(\Delta K + 1)}{\sqrt{(B^{-1})_{\eta_{Z_\alpha}}}}\right], \qquad (10)$$

TABLE II. The same as in Table I, but for heavier nuclei.

Nucleus	K^π	E (MeV)	S_α	$T^{\alpha}_{1/2}$ (th.) (s)	$T^{\alpha}_{1/2}$ (exp.) (s)	$T^{sf}_{1/2}$ (th.) (s)	$T^{sf}_{1/2}$ (exp.) (s)
^{262}Rf	(0^+)	0	9.00×10^{-2}	1.10		6.61	$\geqslant 2.30$
	(8^-)	1.20	8.52×10^{-2}	1.91		6.55×10^{-1}	2.50×10^{-1}
^{266}Hs	(0^+)	0	5.24×10^{-2}	5.44×10^{-3}	3.95×10^{-3}	6.11×10^{-2}	1.25×10^{-2}
	(8^-)	1.20	8.75×10^{-2}	1.08	$74^{+354}_{-34} \times 10^{-3}$	5.25×10^{-2}	
	(18^+)	2.40	9.40×10^{-3}	9.17×10^{3}		1.11×10^{-2}	
^{270}Ds	(0^+)	0	9.25×10^{-2}	8.10×10^{-5}	$10^{+14}_{-4} \times 10^{-5}$	1.59×10^{-2}	$>10^{-3}$ [107]
	(8^+)	1.39	9.01×10^{-2}	4.90×10^{-2}	$7.06^{+16.47}_{-4.71} \times 10^{-3}$	8.15×10^{-3}	$7.06^{+16.47}_{-4.71} \times 10^{-3}$
	(6^+)	1.13	9.15×10^{-2}	1.51×10^{-2}		1.37×10^{-2}	

TABLE III. The calculated (th.) and experimental (exp.) SF ($T^{\rm sf}_{1/2}$) and α-decay ($T^{\alpha}_{1/2}$) half-lives for the ground states ($E=0$) and K-isomers with the excitation energies E in even-odd nuclei. The calculated spectroscopic factors S_α for the α particle are also presented. The experimental data are either from Ref. [12] or indicated references. The values of $T^{\rm sf}_{1/2}$ (exp.) for ^{253}Rf are different in Refs. [48,49] because of different assignments of K to the ground and isomeric states.

Nucleus	K^π	E (MeV)	S_α	$T^{\alpha}_{1/2}$ (th.) (s)	$T^{\alpha}_{1/2}$ (exp.) (s)	$T^{\rm sf}_{1/2}$ (th.) (s)	$T^{\rm sf}_{1/2}$ (exp.) (s)
^{243}Cm	$\frac{5}{2}^+$	0	5.26×10^{-2}	3.81×10^{8}	9.21×10^{8}	2.57×10^{18}	1.73×10^{19}
	$\frac{1}{2}^+$	0.087	7.42×10^{-2}	1.30×10^{6}		2.27×10^{12}	
^{249}No	$(\frac{7}{2}^+)$	0	8.60×10^{-2}	3.14×10^{-2}	1.50×10^{-2}	57	>19 [48]
	$(\frac{1}{2}^+)$	0.100	4.96×10^{-2}	3.41×10^{-3}		0.4	
^{251}No	$(\frac{7}{2}^+)$	0	7.14×10^{-2}	7.59		346	571 [48]
	$(\frac{1}{2}^+)$	0.106	8.81×10^{-2}	1.31×10^{-1}		6.6	
^{255}No	$(\frac{1}{2}^+)$	0	3.33×10^{-2}	3.17×10^{2}	7.04×10^{2}	1.48×10^{4}	
	$(\frac{11}{2}^+)$	0.270	4.29×10^{-2}	6.24×10^{5}		3.27×10^{6}	
	$(\frac{21}{2}^+)$	1.50	2.21×10^{-2}	3.12×10^{4}		8.77×10^{3}	
^{253}Rf	$(\frac{7}{2}^+)$	0	4.41×10^{-2}	0.84×10^{-2}	2.20×10^{-2}	8.6×10^{-3}	$14.6^{+7.0}_{-3.4}\times10^{-3}$ [48]
	$(\frac{1}{2}^+)$	0					$52.8^{+4.4}_{-4.4}\times10^{-6}$ [49]
	$(\frac{1}{2}^+)$	0.200	5.23×10^{-2}	4.1×10^{-3}	6.00×10^{-3}	29.0×10^{-6}	$44^{+17}_{-10}\times10^{-6}$ [48]
	$(\frac{7}{2}^+)$	0.200					$9.9^{+1.2}_{-1.2}\times10^{-3}$ [49]
^{255}Rf	$(\frac{7}{2}^+)$	0	6.91×10^{-2}	11	4	2	2.9
	$(\frac{1}{2}^+)$	0.140	4.07×10^{-2}	2.94×10^{-2}		2.44×10^{-2}	$>5^{+1.7}_{-1.7}\times10^{-5}$ [44]
^{257}Rf	$(\frac{1}{2}^+)$	0	8.67×10^{-2}	1.24	5.55	382	338
	$(\frac{7}{2}^+)$	0.073	1.59×10^{-2}	21.90	5.40	1.07×10^{3}	1.09×10^{3}
	$(\frac{21}{2}^+)$	1.0832	2.13×10^{-2}	8.90×10^{3}		270	
^{261}Rf	$(\frac{3}{2}^+)$	0	9.17×10^{-2}	9.84×10^{-2}		3.2×10^{-2}	
	$(\frac{11}{2}^-)$	0.100	8.91×10^{-2}	3.44		6.10	3.17
^{259}Sg	$(\frac{11}{2}^+)$	0	8.63×10^{-2}	2.51×10^{-1}		1.95	$>1.4\times10^{-3}$
	$(\frac{9}{2}^+)$	~0	6.83×10^{-2}	2.28×10^{-1}		9.72	8
^{265}Sg	$(\frac{9}{2}^+)$	0	8.71×10^{-2}	1.39		872	$\geqslant 17$ [107]
	$(\frac{3}{2}^+)$	0.070	8.33×10^{-2}	4.85	≈17.6	42	≈17.6

where $(B^{-1})_{\eta_{Z_\alpha}}$ is the mass parameter of the DNS with α particle, $T^{\rm sf\text{-}gs}_{1/2}$ is the SF half-life of the ground state with the $K_{\rm gs}$, and $\Delta K = K - K_{\rm gs}$. The parameters ($c_1 = -0.65$, $c_2 = 2.72\times 10^{-3}$), ($c_1 = -0.88$, $c_2 = 1.96\times10^{-2}$), and ($c_1 = -0.88$, $c_2 = -1.97\times10^{-3}$) are suitable in the case of even-even nuclei, odd-A nuclei with $K > K_{\rm gs}$, and odd-A nuclei with $K < K_{\rm gs}$, respectively. As seen in Table IV, the expression (10) with corresponding values of c_1 and c_2 describes the half-lives quite satisfactorily. Based on Eq. (10), the HF for SF from the isomeric state can be estimated. Note that the value of $(B^{-1})_{\eta_{Z_\alpha}}$ weakly depends on nucleus in Table IV.

IV. SUMMARY

Within the cluster model, α decay and SF from the K-isomeric and ground states of both even-even and even-odd nuclei were simultaneously described with the same set of parameters. The calculated results are consistent with the available experimental data. The main assumption of the model is that the charge asymmetry, as the corresponding collective coordinate, is responsible for these decay processes. The spin $\Omega = K$ and energy E of K-isomer modify both the shape and height of fission barrier in η_Z in comparison to the ground-state fission barrier and change SF and α-decay half-lives. Since our model describes well the lifetimes of isomeric states with respect to α decay and SF, then with this model we can try to extract the spins of isomer and ground state from the experimental values of $T^{\alpha,\rm sf}_{1/2}$.

Since the value of $T^{\rm sf}_{1/2}$ of isomeric state decreases with increasing E, but increases with K, then for some E and K this $T^{\rm sf}_{1/2}$ can be smaller than the half-life of α decay and closer to the value of half-life of the electromagnetic decay of the isomeric state. As seen from our calculations, $T^{\rm sf}_{1/2} < T^{\alpha}_{1/2}$ for the isomeric states of even-even nuclei and, correspondingly, the SF and γ-transitions may be the main competing processes. For many isomeric states of odd-A nuclei considered, $T^{\rm sf}_{1/2} \geqslant T^{\alpha}_{1/2}$ and a reason for FH is similar to that for odd-A nuclei in the ground state. The centrifugal potential strongly affects the shape of the driving potential in the region of

TABLE IV. SF half-lives $T_{1/2}^{\text{sf-K}}$ of the isomeric states (K, E) calculated with Eq. (10) in comparison with the theoretical $T_{1/2}^{\text{sf}}$ calculated with Eq. (8). SF half-lives $T_{1/2}^{\text{sf-gs}}$ and values of K_{gs} in the ground state of fissioning nuclei are also indicated.

Nucleus	K_{gs}	K	E (MeV)	$(B^{-1})_{\eta_{Z_\alpha}}$ (MeV s^{-2})	$T_{1/2}^{\text{sf-gs}}$ (s)	$T_{1/2}^{\text{sf-K}}$ (s)	$T_{1/2}^{\text{sf}}$ (s)
^{250}No	0	6	1.050	1.79×10^{-3}	7.02×10^{-5}	7.84×10^{-6}	22.0×10^{-6}
^{252}No	0	8	1.255	1.76×10^{-3}	29.40	0.86	0.20
^{254}No	0	8	1.297	1.74×10^{-3}	6.55×10^{4}	8.98×10^{2}	14.10×10^{2}
^{254}Rf	0	8	1.100	1.74×10^{-3}	3.45×10^{-5}	1.03×10^{-5}	11.40×10^{-5}
^{256}Rf	0	7	1.400	1.71×10^{-3}	4.98×10^{-3}	4.22×10^{-6}	17.80×10^{-6}
^{257}Rf	$\frac{1}{2}$	$\frac{7}{2}$	0.073	1.70×10^{-3}	3.82×10^{2}	1.46×10^{3}	1.07×10^{3}
^{261}Rf	$\frac{3}{2}$	$\frac{11}{2}$	0.100	1.66×10^{-3}	3.22×10^{-2}	3.41	6.10
^{249}No	$\frac{7}{2}$	$\frac{1}{2}$	0.100	1.80×10^{-3}	57.00	0.39	0.40
^{251}No	$\frac{7}{2}$	$\frac{1}{2}$	0.106	1.77×10^{-3}	3.46×10^{2}	2.39	6.60
^{253}Rf	$\frac{7}{2}$	$\frac{1}{2}$	0.200	1.75×10^{-3}	8.60×10^{-3}	5.90×10^{-5}	2.90×10^{-5}
^{255}Rf	$\frac{7}{2}$	$\frac{1}{2}$	0.140	1.72×10^{-3}	2.00	1.37×10^{-2}	2.44×10^{-2}
^{265}Sg	$\frac{9}{2}$	$\frac{3}{2}$	0.070	1.62×10^{-3}	8.72×10^{2}	5.94	42.00

asymmetric DNS, especially for the DNS with α-particle, and, correspondingly, affects the values of SF and α-decay half-lives. Because $K < K_{gs}$ in the K-isomers of ^{249,251}No and ^{253,255}Rf, the SF half-lives for isomeric states are smaller than those for the corresponding ground states. As shown, the SF half-life of the $K^\pi = 6^+$ isomer in ^{250}No is comparable with that of the ground state and perhaps with the half-life of internal electromagnetic transition to the ground state. The SF half-lives of the second K-isomers in the nuclei ^{250,252,254}No and ^{254,256}Rf are also predicted. For example, we obtain $T_{1/2}^{\text{sf}} = 1.5$ μs for $K = 16^+$ isomeric state in ^{250}No which is smaller by about one order of magnitude than the half-life of the ground state. As shown, in ^{254}Rf the isomeric state is more stable against SF than the corresponding ground state. For the SHN ^{266}Hs and ^{270}Ds, the half-lives of the isomeric and ground states are almost comparable.

ACKNOWLEDGMENTS

This work was partly supported by the Ministry of Science and Higher Education of the Russian Federation (Contract No. 075-10-2020-117) and a Tomsk Polytechnic University Competitiveness Enhancement Program grant.

[1] P. M. Walker and G. D. Dracoulis, Nature (London) **399**, 35 (1999).
[2] A. Aprahamian and Y. Sun, Nat. Phys. **1**, 81 (2005).
[3] P. G. Thirolf, S. Kraemer, D. Moritz, and K. Scharl, Eur. Phys. J. Spec. Top. **233**, 1113 (2024).
[4] S. A. Karamian, J. J. Carroll, S. Iliev, and S. P. Tretyakova, Phys. Rev. C **75**, 057301 (2007).
[5] R.-D. Herzberg and P. T. Greenlees, Prog. Part. Nucl. Phys. **61**, 674 (2008).
[6] C. Theisen *et al.*, Nucl. Phys. A **944**, 333 (2015).
[7] F. G. Kondev, G. D. Dracoulis, and T. Kibédi, At. Data Nucl. Data Tables **103**, 50 (2015).
[8] R. M. Clark, Eur. Phys. J. Web Conf. **131**, 02002 (2016).
[9] G. D. Dracoulis, P. M. Walker, and F. G. Kondev, Rep. Prog. Phys. **79**, 076301 (2016).
[10] D. Ackermann and C. Theisen, Phys. Scr. **92**, 083002 (2017).
[11] P. Walker and Z. Podolyák, Phys. Scr. **95**, 044004 (2020).
[12] F. G. Kondev, M. Wang, W. J. Huang, S. Naimi, and G. Audi, Chin. Phys. C **45**, 030001 (2021); S. Garg, B. Maheshwari, B. Singh, Y. Sun, A. Goel, and A. K. Jain, At. Data Nucl. Data Tables **150**, 101546 (2023).
[13] F. P. Hessberger, arXiv:2309.10468.
[14] Z. Podolyák, Eur. Phys. J. Spec. Top. **233**, 903 (2024).
[15] D. L. Balabanski and W. Luo, Eur. Phys. J. Spec. Top. **233**, 1161 (2024).
[16] J. J. Carroll and C. J. Chiara, Eur. Phys. J. Spec. Top. **233**, 1151 (2024).
[17] Y. A. Litvinov and W. Korten, Eur. Phys. J. Spec. Top. **233**, 1191 (2024).
[18] F. R. Xu, X. M. Fu, W. Y. Liang, and Z. Y. Meng, Eur. Phys. J. Spec. Top. **233**, 1047 (2024).
[19] R. M. Clark, Eur. Phys. J. Spec. Top. **233**, 1007 (2024).
[20] P. M. Walker and F. G. Kondev, Eur. Phys. J. Spec. Top. **233**, 983 (2024).
[21] D. Ackermann, S. Antalic, and F. P. Heßberger, Eur. Phys. J. Spec. Top. **233**, 1017 (2024).
[22] A. Ghiorso, K. Eskola, P. Eskola, and M. Nurmia, Phys. Rev. C **7**, 2032 (1973).
[23] Yu. A. Lazarev, Yu. V. Lobanov, R. N. Sagaidak, V. K. Utyonkov, M. Hussonnois, Yu. P. Kharitonov, I. V. Shirokovsky, S. P. Tretyakova, and Yu. Ts. Oganessian, Phys. Scr. **39**, 422 (1989).
[24] H. L. Hall *et al.*, Phys. Rev. C **39**, 1866 (1989).
[25] S. Hofmann *et al.*, Eur. Phys. J. A **10**, 5 (2001).
[26] Yu. Ts. Oganessian *et al.*, Phys. Rev. C **64**, 054606 (2001).
[27] R.-D. Herzberg *et al.*, Nature (London) **442**, 896 (2006).

[28] S. K. Tandel *et al.*, Phys. Rev. Lett. **97**, 082502 (2006).
[29] D. Peterson, B. B. Back, R. V. F. Janssens, T. L. Khoo, C. J. Lister, D. Seweryniak, I. Ahmad, M. P. Carpenter, C. N. Davids, A. A. Hecht, C. L. Jiang, T. Lauritsen, X. Wang, S. Zhu, F. G. Kondev, A. Heinz, J. Qian, R. Winkler, P. Chowdhury, S. K. Tandel *et al.*, Phys. Rev. C **74**, 014316 (2006).
[30] B. Sulignano *et al.*, Eur. Phys. J. A **33**, 327 (2007).
[31] P. T. Greenlees *et al.*, Phys. Rev. C **78**, 021303(R) (2008).
[32] A. P. Robinson *et al.*, Phys. Rev. C **78**, 034308 (2008).
[33] F. P. Heßberger *et al.*, Eur. Phys. J. A **43**, 55 (2010).
[34] B. Streicher *et al.*, Eur. Phys. J. A **45**, 275 (2010).
[35] M. Asai, K. Tsukada, H. Haba, Y. Ishii, T. Ichikawa, A. Toyoshima, T. Ishii, Y. Nagame, I. Nishinaka, Y. Kojima, and K. Sueki, Phys. Rev. C **83**, 014315 (2011).
[36] A. P. Robinson *et al.*, Phys. Rev. C **83**, 064311 (2011).
[37] S. Antalic *et al.*, Eur. Phys. J. A **47**, 62 (2011).
[38] B. Sulignano *et al.*, Phys. Rev. C **86**, 044318 (2012).
[39] J. Rissanen *et al.*, Phys. Rev. C **88**, 044313 (2013).
[40] H. M. David *et al.*, Phys. Rev. Lett. **115**, 132502 (2015).
[41] S. Antalic *et al.*, Eur. Phys. J. A **51**, 41 (2015).
[42] A. I. Svirikhin *et al.*, Phys. Part. Nucl. Lett. **14**, 571 (2017).
[43] J. Kallunkathariyil *et al.*, Phys. Rev. C **101**, 011301(R) (2020).
[44] P. Mosat *et al.*, Phys. Rev. C **101**, 034310 (2020).
[45] K. Kessaci *et al.*, Phys. Rev. C **104**, 044609 (2021).
[46] T. Goigoux *et al.*, Eur. Phys. J. A **57**, 321 (2021).
[47] J. Khuyagbaatar *et al.*, Phys. Rev. C **103**, 064303 (2021).
[48] J. Khuyagbaatar *et al.*, Phys. Rev. C **104**, L031303 (2021).
[49] A. Lopez-Martens *et al.*, Phys. Rev. C **105**, L021306 (2022).
[50] A. Bronis, F. P. Heßberger, S. Antalic, B. Andel, D. Ackermann, S. Heinz, S. Hofmann, J. Khuyagbaatar, B. Kindler, I. Kojouharov, P. Kuusiniemi, M. Leino, B. Lommel, R. Mann, K. Nishio, A. G. Popeko, B. Streicher, B. Sulignano, J. Uusitalo, M. Venhart, and A. V. Yeremin, Phys. Rev. C **106**, 014602 (2022).
[51] J. Khuyagbaatar *et al.*, Phys. Rev. C **106**, 024309 (2022).
[52] K. Hauschild *et al.*, Eur. Phys. J. A **58**, 6 (2022).
[53] M. S. Tezekbayeva *et al.*, Eur. Phys. J. A **58**, 52 (2022).
[54] R. S. Mukhin *et al.*, Chin. Phys. C **48**, 064002 (2024).
[55] A. Lopez-Martens *et al.*, Eur. Phys. J. Web Conf. **290**, 02027 (2023).
[56] C. J. Gallagher and V. G. Soloviev, K. Danske. Vidensk. Selsk. Skr. **2**, 2 (1962).
[57] V. G. Solov'ev, A. V. Sushkov, and A. Yu. Shirikova, Sov. J. Nucl. Phys. **54**, 748 (1991).
[58] F. R. Xu, E. G. Zhao, R. Wyss, and P. M. Walker, Phys. Rev. Lett. **92**, 252501 (2004).
[59] A. Parkhomenko and A. Sobiczewski, Acta Phys. Pol. B **35**, 2447 (2004); **36**, 3095 (2005); **36**, 3115 (2005).
[60] J.-P. Delaroche, M. Girod, H. Goutte, and J. Libert, Nucl. Phys. A **771**, 103 (2006).
[61] G. G. Adamian, N. V. Antonenko, and W. Scheid, Phys. Rev. C **81**, 024320 (2010); G. G. Adamian, N. V. Antonenko, S. N. Kuklin, and W. Scheid, *ibid.* **82**, 054304 (2010).
[62] G. G. Adamian, N. V. Antonenko, S. N. Kuklin, B. N. Lu, L. A. Malov, and S. G. Zhou, Phys. Rev. C **84**, 024324 (2011).
[63] H. L. Liu, F. R. Xu, and P. M. Walker, Phys. Rev. C **86**, 011301(R) (2012).
[64] P. M. Walker, F. R. Xu, and H. L. Liu, J. Phys. G: Nucl. Part. Phys. **39**, 105106 (2012).
[65] A. N. Kuzmina, G. G. Adamian, and N. V. Antonenko, Phys. Rev. C **85**, 017302 (2012); **85**, 027308 (2012).
[66] H. L. Liu, P. M. Walker, and F. R. Xu, Phys. Rev. C **89**, 044304 (2014).
[67] A. N. Bezbakh, V. G. Kartavenko, G. G. Adamian, N. V. Antonenko, and R. V. Jolos, and V. O. Nesterenko, Phys. Rev. C **92**, 014329 (2015).
[68] V. Prassa, Bing-Nan Lu, T. Niksic, D. Ackermann, and D. Vretenar, Phys. Rev. C **91**, 034324 (2015).
[69] P. Jachimowicz, M. Kowal, and J. Skalski, Phys. Rev. C **92**, 044306 (2015).
[70] G. G. Adamian, N. V. Antonenko, A. N. Bezbakh, and R. V. Jolos, Phys. Part. Nuclei **47**, 387 (2016).
[71] G. G. Adamian, N. V. Antonenko, L. A. Malov, and H. Lenske, Phys. Rev. C **96**, 044310 (2017); G. G. Adamian, N. V. Antonenko, H. Lenske, L. A. Malov, and S.-G. Zhou, Eur. Phys. J. A **57**, 89 (2021).
[72] W. Brodzinski, M. Kowal, J. Skalski, and P. Jachimowicz, Acta Phys. Pol. B **49**, 621 (2018).
[73] N. Minkov, L. Bonneau, P. Quentin, J. Bartel, H. Molique, and D. Ivanova, Phys. Rev. C **105**, 044329 (2022).
[74] W. M. Seif and A. R. Abdulghany, Phys. Rev. C **108**, 024308 (2023).
[75] L. A. Malov, A. N. Bezbach, G. G. Adamian, N. V. Antonenko, and R. V. Jolos, Phys. Rev. C **106**, 034302 (2022); **108**, 044302 (2023).
[76] W. M. Seif and A. R. Abdulghany, Phys. Rev. C **109**, 044326 (2024).
[77] Yu. T. Oganessian, J. Phys. G **34**, R165 (2007).
[78] Yu. T. Oganessian and V. K. Utyonkov, Nucl. Phys. A **944**, 62 (2015); Rep. Prog. Phys. **78**, 036301 (2015).
[79] S. Hofmann and G. Münzenberg, Rev. Mod. Phys. **72**, 733 (2000).
[80] S. Hofmann *et al.*, Eur. Phys. J. A **52**, 116 (2016); **52**, 180 (2016).
[81] J. Khuyagbaatar, Eur. Phys. J. A **58**, 243 (2022).
[82] I. S. Rogov, G. G. Adamian, and N. V. Antonenko, Phys. Rev. C **100**, 024606 (2019).
[83] I. S. Rogov, G. G. Adamian, and N. V. Antonenko, Phys. Rev. C **104**, 034618 (2021).
[84] I. S. Rogov, G. G. Adamian, and N. V. Antonenko, Phys. Rev. C **105**, 034619 (2022).
[85] Yu. T. Oganessian *et al.*, Phys. Rev. C **106**, 064306 (2022).
[86] Yu. T. Oganessian *et al.*, Phys. Rev. C **108**, 024611 (2023).
[87] Yu. T. Oganessian *et al.*, Phys. Rev. C **109**, 054307 (2024).
[88] R. K. Gupta, S. Singh, R. K. Puri, and W. Scheid, Phys. Rev. C **47**, 561 (1993).
[89] Yu. M. Tchuvil'sky, *Cluster Radioactivity* (Moscow State University, Moscow, 1997).
[90] W. Greiner, M. Ivascu, D. N. Poenaru, and A. Sandulescu, in *Treatise on Heavy Ion Science*, edited by D. A. Bromley (Plenum, New York, 1989), Vol. 8, p. 641.
[91] Yu. S. Zamyatnin *et al.*, Sov. J. Part. Nucl. **21**, 231 (1990).
[92] S. G. Kadmensky, S. D. Kurgalin, and Yu. M. Tchuvil'sky, Phys. Part. Nuclei **38**, 699 (2007).
[93] D. N. Poenaru, *Nuclear Decay Modes* (IOP Publishing, Bristol, 1996).
[94] K. Varga, R. G. Lovas, and R. J. Liotta, Phys. Rev. Lett. **69**, 37 (1992).
[95] N. Itagaki, J. Cseh, and M. Ploszajczak, Phys. Rev. C **83**, 014302 (2011).

[96] J. Cseh, A. Algora, J. Darai, and P. O. Hess, Phys. Rev. C **70**, 034311 (2004); A. Algora, J. Cseh, J. Darai, and P. O. Hess, Phys. Lett. B **639**, 451 (2006).

[97] W. Sciani, Y. Otani, A. Lépine-Szily, E. A. Benjamim, L. C. Chamon, R. L. Filho, J. Darai, and J. Cseh, Phys. Rev. C **80**, 034319 (2009); J. Cseh, J. Darai, W. Sciani, Y. Otani, A. Lépine-Szily, E. A. Benjamim, L. C. Chamon, and R. L. Filho, *ibid.* **80**, 034320 (2009).

[98] D. Lebhertz *et al.*, Phys. Rev. C **85**, 034333 (2012).

[99] S. N. Kuklin, G. G. Adamian, and N. V. Antonenko, Yad. Fiz. **68**, 1501 (2005); Phys. At. Nucl. **68**, 1443 (2005); Phys. Rev. C **71**, 014301 (2005); Yad. Fiz. **71**, 1788 (2008); Phys. At. Nucl. **71**, 1756 (2008); S. N. Kuklin, T. M. Shneidman, G. G. Adamian, and N. V. Antonenko, Eur. Phys. J. A **48**, 112 (2012).

[100] G. G. Adamian, N. V. Antonenko, and W. Scheid, in *Clusters in Nuclei*, Lecture Notes in Physics, Vol. 848, edited by C. Beck (Springer-Verlag, Berlin, 2012), p. 165.

[101] G. G. Adamian *et al.*, Int. J. Mod. Phys. E **05**, 191 (1996).

[102] J. K. Tuli, *Nuclear Wallet Cards* (BNL, New York, NY, 2000).

[103] P. Jachimowicz, M. Kowal, and J. Skalski, At. Data Nucl. Data Tables **138**, 101393 (2021).

[104] P. Möller, A. J. Sierk, T. Ichikawa, and H. Sagawa, At. Data Nucl. Data Tables **109**, 1 (2016).

[105] T. M. Shneidman, G. G. Adamian, N. V. Antonenko, R. V. Jolos, and W. Scheid, Phys. Lett. B **526**, 322 (2002); Phys. Rev. C **67**, 014313 (2003); **70**, 064318 (2004).

[106] S. Raman *et al.*, At. Data Nucl. Data Tables **78**, 1 (2001).

[107] F. P. Heßberger, Eur. Phys. J. A **53**, 75 (2017).